World Journal of Microbiology and Biotechnology (2023) 39:170
https://doi.org/10.1007/s11274-023-03618-z

RESEARCH

Transcriptional analysis of the dimorphic fungus *Umbilicaria muehlenbergii* reveals the molecular mechanism of phenotypic transition

Dongjie Fan[1] · Lushan Liu[2] · Shunan Cao[3] · Rui Liao[4] · Chuanpeng Liu[5] · Qiming Zhou[4]

Received: 2 July 2022 / Accepted: 13 April 2023 / Published online: 26 April 2023

Abstract

The lichen-forming fungus *Umbilicaria muehlenbergii* undergoes a phenotypic transition from a yeast-like to a pseudohyphal form. However, it remains unknown if a common mechanism is involved in the phenotypic switch of *U. muehlenbergii* at the transcriptional level. Further, investigation of the phenotype switch molecular mechanism in *U. muehlenbergii* has been hindered by incomplete genomic sequencing data. Here, the phenotypic characteristics of *U. muehlenbergii* were investigated after cultivation on several carbon sources, revealing that oligotrophic conditions due to nutrient stress (reduced strength PDA (potato dextrose agar) media) exacerbated the pseudohyphal growth of *U. muehlenbergii*. Further, the addition of sorbitol, ribitol, and mannitol exacerbated the pseudohyphal growth of *U. muehlenbergii* regardless of PDA medium strength. Transcriptome analysis of *U. muehlenbergii* grown in normal and nutrient-stress conditions revealed the presence of several biological pathways with altered expression levels during nutrient stress and related to carbohydrate, protein, DNA/RNA and lipid metabolism. Further, the results demonstrated that altered biological pathways can cooperate during pseudohyphal growth, including pathways involved in the production of protectants, acquisition of other carbon sources, or adjustment of energy metabolism. Synergistic changes in the functioning of these pathways likely help *U. muehlenbergii* cope with dynamic stimuli. These results provide insights into the transcriptional response of *U. muehlenbergii* during pseudohyphal growth under oligotrophic conditions. Specifically, the transcriptomic analysis indicated that pseudohyphal growth is an adaptive mechanism of *U. muehlenbergii* that facilitates its use of alternative carbon sources to maintain survival.

Keywords Filamentous growth · Next-generation sequencing · Pseudohyphea · Transcriptome

✉ Chuanpeng Liu
liucp74@hotmail.com

✉ Qiming Zhou
genbank@vip.sina.com

[1] State Key Laboratory of Infectious Disease Prevention and Control, Collaborative Innovation Center for Diagnosis and Treatment of Infectious Diseases, National Institute for Communicable Disease Control and Prevention, Chinese Center for Disease Control and Prevention, Beijing 102206, China

[2] Emergency Department of China Rehabilitation Research Center, Capital medical University, Fengtai District, No. 10 Jiaomen North Street, Beijing 100068, China

[3] Key Laboratory for Polar Science MNR, Polar Research Institute of China, NO.1000 Xuelong Road, Pudong, Shanghai, China

[4] ChosenMed Technology Company Limited, Economic and Technological Development Area, Jinghai Industrial Park, No. 156 Fourth Jinghai Road, Beijing, China

[5] School of Life Science and Technology, Harbin Institute of Technology, 92 West Dazhi Street, Harbin 150080, China

Introduction

Lichens are composite organisms comprising algae or cyanobacteria that live among fungal filaments via symbiotic relationships and are often found in extreme environments like deserts and cold polar regions. Algae or cyanobacteria in lichens are termed photobionts, while fungi are considered mycobionts. Complicated symbiotic relationships exist between lichen-forming mycobionts and their algal partners (photobionts). For example, photobionts can produce carbohydrates that support mycobiont metabolism in lichens (Palmqvist 2000), including various carbohydrates like glucose, ribitol, erythritol, and sorbitol (Aubert et al. 2007; Richardson et al. 1967; Spribille et al. 2022). Further, the mycobionts protect photobionts from harsh environmental conditions and are responsible for producing secondary metabolites that exhibit antioxidant, radio resistance, and antimicrobial activities including alkaloids, polyketides, and terpenes (Molnar and Farkas 2010; Zakeri et al. 2022). Some secondary metabolites or derivatives from lichen-forming fungi exhibit diverse biological properties including antimicrobial, antiviral, and antitumor activities (Hirabayashi et al. 1989; Stepanenko. et al. 1998). In addition, the secondary metabolite profiles from lichenized fungi are dependent on the type and concentration of carbohydrates received from algae as carbon sources (Brunauer et al. 2006, 2007). For example, lower concentrations of the carbon sources glucose, sorbitol, and ribitol in media can promote polyketide production (Elshobary et al. 2016).

Some fungi, including *Candida albicans*, *Histoplasma capsulatum*, *Blastomyces dermatitidis*, *Paracoccidioides brasiliensis*, and *Saccharomyces cerevisiae* can naturally undergo phenotype switches, in which their morphologies change from yeast-like to hyphal or pseudohyphal forms. The phenotype switches are affected by environmental and nutritional stresses and are even required to achieve virulence in the pathogenic fungus *Candida albicans* (Madhani 2000; Lorenz et al. 2000). Phenotype switches have been extensively studied in the model fungus *Saccharomyces cerevisiae*, which displays three cellular morphologies during development: yeast, pseudohyphae, and hyphae. The filamentous growth of *Saccharomyces cerevisiae* is controlled by a regulatory network encompassing mitogen-activated protein kinase (MAPK), cAMP-dependent protein kinase A (PKA), Elm1p, and Snf1p kinase (Cullen et al. 2004; Kuchin et al. 2002; Karunanithi et al. 2010; Pan and Heitman 1999). Furthermore, extensively phosphorylated proteins that depend on these kinases also control yeast pseudohyphal growth at the proteomic level (Shively et al. 2015). Moreover, previous studies have indicated that approximately 700 genes involved in various biological pathways are required for *Saccharomyces cerevisiae* pseudohyphal growth (Jin et al. 2008; Ryan et al. 2012).

Umbilicaria muehlenbergii belongs to the order *Umbilicariales*, whose members exhibit circle leaf-shaped thalli and a unique umbilicus (i.e., a navel) that attaches to substrates. The mycobiont *U. muehlenbergii* is the first reported dimorphic lichen-forming fungus. Compared to most other lichen-forming fungi that are slow-growing, *U. muehlenbergii* is relatively fast-growing when cultured in the yeast form. However, *U. muehlenbergii* also exhibits pseudohyphal forms under some stressful conditions (Park et al. 2013).

Although cAMP signaling has been shown to play a role in regulating the dimorphic transition of *U. muehlenbergii* (Wang et al. 2020), the full scope of biological pathways and genes that regulate the switch between yeast-like and pseudohyphal growth in response to nutrient limitation or stress remain unclear. A draft genome sequence for *U. muehlenbergii* is available (Park et al. 2014). However, the mechanism responsible for the dimorphic switch cannot be interpreted at the DNA level. Rather, transcriptome data is required to identify factors that promote the yeast-to-pseudohypha transition in *U. muehlenbergii*.

RNA sequencing (RNA-seq) has been widely used for transcriptional analysis, gene discovery, and molecular marker development in diverse organisms. Further, the *de novo* sequencing technology has been successfully applied to the investigation of some fungal species without corresponding reference genomes (Liu et al. 2014; Zhang et al. 2013). Consequently, RNA-seq was conducted here to investigate transcriptional responses of *U. muehlenbergii* cultured under normal and oligotrophic conditions. The specific aims of the study were to (1) improve *U. muehlenbergii* genome annotation; (2) identify biological pathways associated with pseudohyphal growth of *U. muehlenbergii* in response to nutrient stress.

Materials and methods

Morphological observations of *U. muehlenbergii* under normal and nutrient-limiting conditions

Yeast-like *U. muehlenbergii* was isolated from sample liu15008 that was collected from Wangqing China in 2014 and was subsequently routinely cultured on 100% potato dextrose broth (PDB) at 25 °C for 3 d, with shaking at 110 rpm. For morphological observations in nutrient-limited conditions, 100 µL yeast-like *U. muehlenbergii* with an OD_{600} of 0.8 were diluted into 1 mL culture, which were vortexed for 15 s. The 2 µl diluted *U. muehlenbergii* culture were inoculated on to 100% strength potato dextrose agar

(PDA) (20 g PDA in 1 L H_2O), 1/3 strength PDA (6.67 g PDA in 1 L H_2O), 1/900 strength PDA (0.022 g PDA in 1 L H_2O), and water-agar medium with 0.1 M final concentrations of different sugars including mannitol, sorbitol, ribitol, glucose, trehalose, and sucrose. The cultures were incubated at 25 °C. *U. muehlenbergii* cultures were then imaged using a Nikon microscope after culturing for 24 h.

Strain cultivation for RNA-sequencing

A 100 µl inoculum of yeast-like *U. muehlenbergii* was inoculated into 100 ml of PDB and then cultured at 25 °C with shaking at 110 rpm in the dark for 3 d. In addition, 500 µl of *U. muehlenbergii* culture in PDB was centrifuged at 4,000 rpm for 2 min at 4 °C. The resultant pellet was further cultured in 100 ml of 1/900 PDB containing 0.1 M D-sorbitol at 25 °C for 24 h with shaking at 110 rpm as stress cultivation. In parallel, 500 µl of *U. muehlenbergii* culture was cultured in the same manner, but grown in 100 ml of normal PDB as the control. Three stress replicates or control replicates, were mixed respectively with quality radio of 1:1:1, and then used for the following RNA extraction.

RNA extraction, library construction, and sequencing

U. muehlenbergii cells cultured with 100% PDB (control) and with 1/900 PDB containing 0.1 M D-sorbitol (oligotrophic culture) were collected by centrifuging at 4,000 rpm for 10 min at 4 °C. Total RNA was then isolated from the cells using the nucleoSpin RNA kit (Macherey-Nagel, Germany). RNA quantity and quality were assessed using an Agilent 2100 Bioanalyzer (Agilent Technologies). RIN values ≥ 8.0 and 28 S/18S values ≥ 1.5 were used as criteria for identifying high quality RNA extracts. Approximately 3 µg of total RNA from each sample was used to prepare libraries. A TruSeq RNA sample preparation kit (Illumina, San Diego, CA) was used to prepare libraries according to the manufacturer's instructions. Briefly, mRNAs containing poly (A) tails were purified from total RNA using poly (T) oligonucleotides attached to magnetic beads. After purification, mRNA was fragmented into 200–700-nt lengths by adding fragmentation buffer and using divalent cation catalysts under increased temperature incubation. Fragmented mRNA was converted to first strand cDNA with reverse transcriptase and random hexamers. Single strand cDNA was then converted to double strand cDNA using DNA polymerase I and RNase H. Double stranded cDNA was then end repaired, ligated with indexing adapters, purified, and enriched via PCR to generate the final library. The prepared libraries were then sequenced on the Illumina HiSeq™ 2000 platform at the BerryGenomics Corporation (Beijing, China). Raw sequencing data are available in the National Centre for Biotechnology Information (NCBI) Sequence Read Archive database under the BioSample accession numbers SAMN27771024 and SAMN27771025.

De novo transcript assembly, functional annotation, and similarity analysis

Raw reads in fastq format were processed and filtered by software cutadapt (v1.14) and Trimmomatic (v0.32) (Marcel 2011; Bolger et al. 2014) with in-house Perl scripts. Then, the clean reads were obtained by removing raw reads containing adapter sequences, reads containing poly-N bases, and low-quality reads. The Q20, GC-content, and sequence duplication level metrics were calculated for the clean data. All downstream analyses were then based on high-quality clean data. The Trinity program was used to assemble the clean reads into contigs that were then assembled into unigenes. The assembled unigenes were compared against the NCBI non-redundant protein sequence database (Nr), the Annotated and Reviewed Protein Sequence database (Swiss-Prot), the Clusters of Orthologous Groups of proteins database (COG), and the Kyoto Encyclopedia of Genes and Genomes database (KEGG) using BLASTx with an E-value cut-off of 10^{-5}. Unigene direction was determined based on the orientation of the highest matched protein among the four databases. For unigenes without defined annotation using BLASTX, their unigene direction was determined using the ESTscan software program.

The assembled *U. muehlenbergii* unigenes were subjected to BLASTX analysis against the NCBI non-redundant protein sequence database (Nr) to evaluate sequence conservation among fungal species.

Simple sequence repeats (SSRs) identification and gene ontology (GO) enrichment analysis of SSRs-containing transcripts

To detect SSRs markers, unigene sequences containing 2–6 repeat motifs were identified using the MISA server (http://pgrc.ipk-gatersleben.de/misa/). SSR motif detection parameters were set to default settings. GO enrichment analysis of the unigene-derived SSRs were performed using the OmicShare tools, an online platform for data analysis (https://www.omicshare.com/tools).

Identification, GO enrichment and KEGG pathway analysis of differentially expressed unigenes

The expression levels of unigenes were calculated based on the Reads Per Kilobase per Million (RPKM) mapped reads metric, calculated as $10^9 \times C/(N \times L)$, where C is the

number of reads uniquely aligned to the unigene; N is the total number of reads aligned to all unigenes; and L is the number of bases in the unigene. The transcript expression levels were calculated using the Fragments Per Kilobase of transcript per Million (FPKM) mapped reads metric that is calculated similarly to RPKM, except that C represents the number of fragments aligned to the transcript, N is the total number of fragments aligned to the reference transcripts, and L is the number of bases in the transcript. Differential gene expression was detected using EdgeR (Robinson et al. 2010), in which the parameter bcv was set to 0.1 in time of called exactTest function. A false discovery rate (FDR) threshold of $P < 0.05$ was used to assess the degree of differences in gene expression. Fold change was determined based on FPKM values among different samples, as $\log_2(FPKM_{nutrient\ stressed}/FPKM_{normal\ culture})$. Transcripts with FDR ≤ 0.05 and Abs (log2(fold change)) ≥ 1 were identified as differentially expressed in the nutrient stressed samples.

GO enrichment of the differentially expressed genes was further analysed by the GOseq R package, in which the unigene length bias was corrected. The GOseq R package calculates the *P*-value through the Wallenius non-central hyper-geometric distribution. GO terms with a corrected *P* value less than 0.05 were considered significantly enriched. KOBAS software (Mao et al. 2005) was also used to test the significance of differentially expressed genes enrichment in the KEGG database (http://www.genome.jp/kegg/).

Results

Medium composition determines *U. muehlenbergii* morphological switches

The *U. muehlenbergii* strain investigated here was obtained from a natural lichen thallus. Pseudohyphal and yeast-like growth forms of *U. muehlenbergii* have been identified based on isolation with solid PDA medium and in liquid PDB medium (Park et al. 2013). To evaluate the effects of nutrient composition on *U. muehlenbergii* growth states, different sugar alcohol, and sugar compounds were added to agar plates at different concentrations, followed by observing *U. muehlenbergii* morphological states. More *U. muehlenbergii* pseudohyphae appeared in medium with decreased PDA contents and under conditions with the presence of certain sugar alcohols or sugar compounds. When cultivated with a 100% PDA medium, the addition of mannitol, glucose, and sucrose minimally affected pseudohyphal growth of *U. muehlenbergii*, while the addition of trehalose, sorbitol, and ribitol prompted increased pseudohyphal growth. Upon dramatic decreases in PDA strength, the morphologic switches of *U. muehlenbergii* were more clearly induced by the addition of different polyols (i.e., sorbitol, mannitol, and ribitol). When cultivated in 1/900 strength PDA with 10% sorbitol, mannitol, and ribitol, pseudohyphae appeared more clearly compared with growth on 1/900 strength PDA with glucose and sucrose (Fig. 1). Thus, cultivation in the PDA medium with the addition of polyols generally led to clearer pseudohyphal phenotypes of *U. muehlenbergii*. Consequently, the lichen fungus *U. muehlenbergii* tends to form pseudohyphae rather than existing in yeast form under oligotrophic conditions. Further, growth on polyols more easily induced pseudohyphal formation of *U. muehlenbergii* compared to growth on glucose and sucrose. To assess the transcriptional regulation of *U. muehlenbergii* in association with the pseudohyphae phenotype in oligotrophic medium, RNA sequencing was conducted when growing the cultures in 100% PDB and reduced PDB containing sorbitol (oligotrophic conditions).

Transcriptomic analysis of *U. muehlenbergii*

Two normalized cDNA libraries recovered from *U. muehlenbergii* cultured in full-strength PDB and oligotrophic conditions were constructed. Transcriptomic assembly statistics are provided in Tables 1 and 2, while unigene numbers and length distributions are shown in Fig. 2. RNA-seq from the two cDNA pools produced a total of 41,954,102 reads and 54,872 high-quality transcripts with an average Q20 rate of 92.93% and GC percentage of 51.65%. N50 values reflect assembly quality based on the distribution of contig lengths; herein, the metric shows the length at which 50% of the total assembled contigs are larger than the N50 value and this metric was calculated based on transcripts representing 90% of the expression data. Thus, larger N50 values indicate better sequencing quality. The N50 value of the assemblies used here was 1,487, with an average contig length of 908.63 bp and a maximum number of unigenes (12,744) in the 200–299 bp size distribution, along with a significantly lower number (2,723) that were ≥ 2,000 bp (Fig. 2). Moreover, the sequenced clean data from two culture condition were both aligned to 18 S rRNA and ITS regions of *U. muehlenbergii* (Genbank No. KY947997.1), and 0.2% clean reads could be aligned perfectly (100% identical) to the sequence from KY947997.1. The average sequencing depths of extracted clean reads with full alignment to 18 S rRNA and ITS regions of *U. muehlenbergii* (KY947997.1) were 559X and 472X for two culture condition, respectively. These metrics suggested the presence of good sequencing quality for the *U. muehlenbergii* genome.

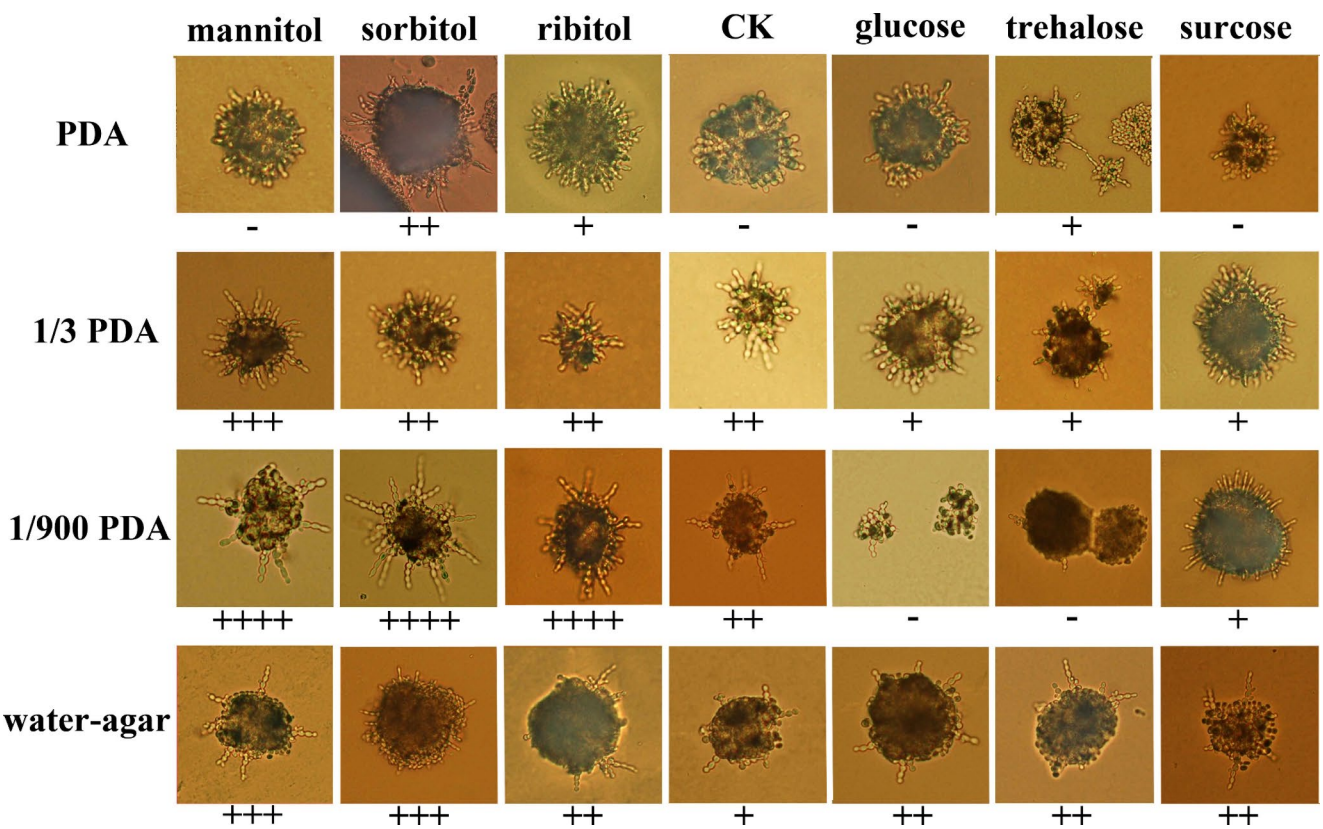

FIg. 1 The effect of PDA strength on morphological switches of *U. muehlenbergii*. The 0.1 M polyols (mannitol, sorbitol and ribitol), trehalose, glucose and sucrose were added into PDA medium as alternative carbon source. In the reduced concentration of PDA (1/3 PDA and 1/900 PDA) medium, addition of sorbitol, mannitol and ribitol could increase pseudohyphal growth of *U. muehlenbergii*. CK means control check, without any alternative carbon source. The number of symbols + means pseudohyphal intensity. The more symbol + indicate that there is the longer and clearer pseudohyphae. The symbol – means there is no clear pseudohyphal growth

Table 1 RNA sequencing summary for *U. muehlenbergii* transcriptomes under normal and oligotrophic culture conditions

	Normal culture	Oligotrophic culture
Total reads (bp)	21,540,446	20,413,656
Total base pairs (bp)	2,692,555,750	2,551,707,000
Total mapped reads (bp)	13,927,622	12,674,390
Percentage of mapped reads	64.66%	62.09%
Total number of raw reads (bp)	11,075,961	10,519,177
Total number of clean reads (bp)	10,770,223	10,206,828
Percentage of clean reads	97.24%	97.03%

Table 2 Summary of the final *U. muehlenbergii* transcriptome assembly

Q20 value	92.93%
GC percentage	51.65%
N50 length (bp)	1,487
Average contig length (bp)	908.63
Total number of unigenes	54,872
Total assembled bases	50,390,794
NCBI Nr annotated	13,406
Swiss-Prot annotated	7,268
KEGG annotated	4,130
COG annotated	4,864
Unigenes with annotation	13,421
Unigenes without annotation	42,037

Unigene annotation and distribution across species

To thoroughly investigate unigene functions, BLASTX was used to align unigenes against the Nr, Swissprot, COG, and KEGG databases. A total of 13,421 annotated genes and 42,037 non-annotated unigenes were identified. Among all unigenes, 13,406 (99.88%), 7,268 (54.15%), 4,864 (36.28%), and 4,130 (30.77%) were annotated to the Nr, Swissprot, COG, and KEGG databases, respectively (Table 2). A total of 2,563 unigenes were annotated in all four databases. Thus, these annotated data considerably aid functional genomic research for *U. muehlenbergii* and help mitigate the paucity of *U. muehlenbergii* draft genomic data.

To investigate sequence conservation between *U. muehlenbergii* and other species, the number of homologous sequences from *U. muehlenbergii* were identified based on BLASTX alignment to other species in the Nr database (Fig. 3). *U. muehlenbergii* unigenes mostly matched those in the genome of *Glarea lozoyensis* ATCC

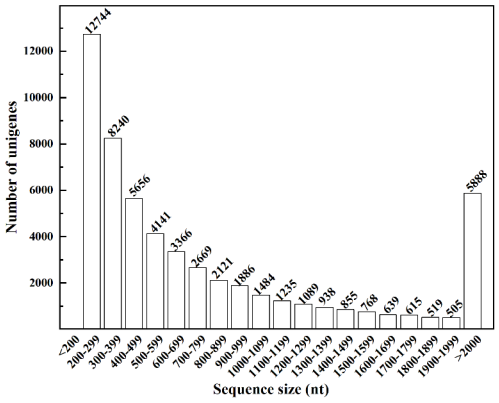

Fig. 2 Length distribution of *U. muehlenbergii* unigenes in base pairs. The numbers of unigenes are shown on top of each bar

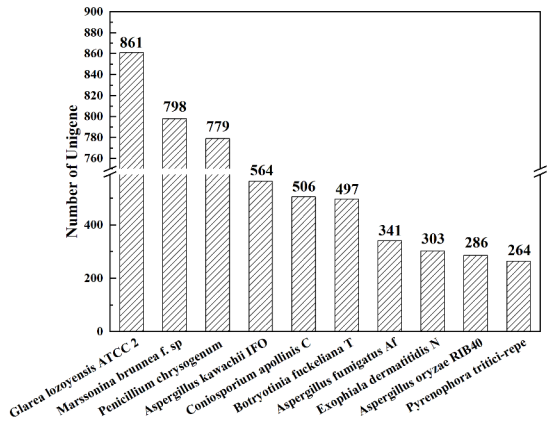

Fig. 3 The sequence similarity between *U. muehlenbergii* and other species was performed by BLASTX (E-value ≤ 1E-05).

20868, which is a filamentous fungus that produces multiple secondary metabolite products. The second most matched genome was that of *Marssonina brunnea f. sp. 'multigermtubi' MB*_m1, a fungal pathogen (Zhu et al. 2012). Other lesser-matched genomes included those of *Penicillium chrysogenum Wisconsin 54-1255*, *Aspergillus kawachii IFO 430*, and *Coniosporium apollinis CBS 100,218*, which are all non-lichen-forming fungi. Some of these strains exhibit the ability to produce penicillin or α-amylase. Filamentous fungi are prolific sources of secondary metabolites that have long been regarded as major sources of therapeutic agents. Sequence conservation analysis overall indicated that *U. muehlenbergii* genes exhibited close homologous relationships with several of the abovementioned fungi that produce secondary metabolites, implying that *U. muehlenbergii* may be a potential resource for discovering novel active natural products.

Distribution of simple sequence repeats markers

RNA-seq could discover and identify simple sequence repeats (SSRs) markers in non-model strains without detailed genomic information. Consequently, the MISA tool was used to identify all the SSRs of *U. muehlenbergii* from coding regions and non-coding regions, referred to unigene-derived SSRs and non-unigene-derived SSRs herein. A total of 2,469 SSRs were identified, representing a frequency of 1 SSRs per 20.41 Kbp. There were 2,187 unigene-derived SSRs, accounting for 88.58% of total SSRs. The existence of higher proportion of unigene-derived SSRs indicated that most of the variations with unique identity and position located in genomic regions of gene activation and protein expression. Among the total identified SSRs, tri-nucleotide repeats comprised the largest fraction (46.98%), followed by hexa-nucleotide repeats (20.49%), tetra-nucleotide repeats (14.5%), penta-nucleotide repeats (9.64%), and di- nucleotide repeats (8.38%) (Table 3). The four most abundant motif repeats were (AGG/CCT)n (7.7%), (AAG/CTT)n (7.5%), (AGC/CTG)n (6.6%), and (ATC/ATG)n (6.1%) (Fig. 4). The proportion and repeat type of SSRs of *U. muehlenbergii* of was probably typical characteristic of SSRs in dimorphic fungi. Higher complexity nucleotide repeat SSRs were observed in progressively smaller numbers, but also still comprised a significant proportion of total SSRs (Table 3). The combined proportion of higher complexity nucleotide repeat SSRs (tetra-, penta- and hexa-nucleotide repeats) were 44.63%, which were close to the combined proportion of lower complexity nucleotide repeat SSRs (di- and tri-nucleotide repeats), which were 55.36%, suggesting that genome of *U. muehlenbergii* was relatively

Table 3 SSR distribution in the *U. muehlenbergii* transcriptome assembly

	Numbers of repeat unit									
Motif length	4	5	6	7	8	9	10	> 10	Total	Frequency (%)
Di	0	0	119	53	15	9	2	9	207	8.38
Tri	0	588	250	150	112	21	16	23	1,160	46.98
Tetra	245	66	36	3	5	0	1	2	358	14.50
Penta	165	57	11	3	0	0	1	1	238	9.64
Hexa	408	49	21	14	4	4	0	6	506	20.49
Total	818	760	437	223	136	34	20	41		
Frequency (%)	33.13	30.78	17.70	9.03	5.51	1.38	0.81	1.66		

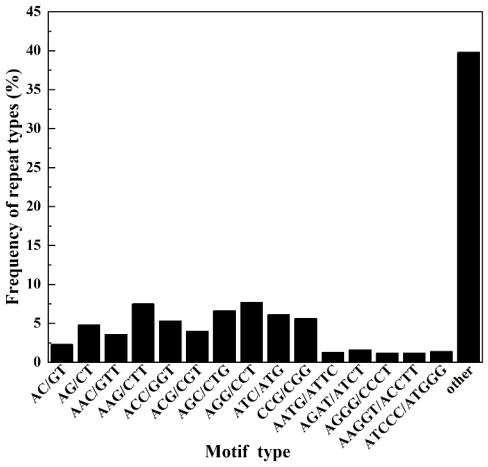

Fig. 4 Frequency distribution of SSRs based on motif types in *U. muehlenbergii*

stable in fungi genome without high mutation frequency and high rate of evolution.

The unigene-derived SSRs were associated with coding regions of identified transcripts with differential expression. Therefore, GO enrichment analysis was applied to unigene-derived SSRs with differential expression (Supplemental Fig. 1 and Table 1). Within the GO-molecular function category, most unigene-derived SSRs were assigned to the transmembrane transporter activity (GO:0022857), followed by some GO term associating with enzymatic activity, such as ligase and oxidoreductase activity. Within the GO-biological pathway category, some unigene-derived SSRs exhibited mitotic cell cycle (GO:0000278), cell death (GO:0008219) and septin ring organization (GO:0031106), that were closely related to cell genesis, division and shape, while another exhibited phosphatidylinositol metabolic process (GO:0046488), which is implicated in cytoskeleton regulation and membrane dynamics. Cellular response to chemical stimulus (GO:0070887) were also enriched with quite a few unigene-derived SSRs, which is implicated in expressional alteration triggered by oligotrophic stress. Apart from them, the GO term associating with carbohydrate metabolism were enriched with a few unigene-derived SSRs, such as monosaccharide catabolic process (GO:0046365), hexose catabolic process (GO:0019320) and glucose catabolic process (GO:0006007). Within the GO-cellular component annotated category, some unigene-derived SSRs were clearly involved in ribonucleoprotein complex (GO:1,990,904) and ribosomal subunit (GO:0044391), as shown in Supplemental Fig. 1. The classified SSRs showed adaptive traits with differential expression under oligotrophic condition, suggesting that they could represent valuable markers for researching pseudohyphal growth.

Exploration and characterization of differentially expressed transcripts

To identify transcriptomic information related to pseudohyphal growth of *U. muehlenbergii* under oligotrophic conditions, the expression levels of transcripts were compared under normal and oligotrophic conditions. A total of 1,718 transcripts were significantly differentially expressed under nutrient stress based on the criteria of FDR ≤ 0.05 and abs(log2 (fold change)) ≥ 1. Among these, 989 were upregulated and 729 were downregulated (Fig. 5) (Supplemental Table 2). The most upregulated transcript was GG8657|c1_g1_i1, which encodes an exoribonuclease phosphorolytic domain 1 of the ribonucleoprotein complex that is involved in RNA degradation (ko03018). The most downregulated transcript was GG4683|c67_g1_i1, which encodes the ubiquitin-40 S ribosomal protein S31 that is part of the ribosome (ko03010). To confirm the reliability of the RNA-seq data, the expression of eight differentially expressed transcripts and one internal control transcript were evaluated with quantitative real-time PCR (RT-PCR). The expression of these transcripts based on RT-PCR was consistent with RNA-seq values, confirming the reliability of the transcriptomic data. RT-PCR methods and results are provided in the Supplemental Material, Supplemental Tables 3 and Supplemental Fig. 2.

GO analysis of transcripts with altered expression

To obtain more comprehensive information on the biological function of transcripts with altered expression related to pseudohyphal growth during oligotrophic stress, transcripts were assigned to GO categories including cellular components, molecular function, and biological processes.

The GO-cellular component analysis clearly indicated that transcripts with altered expression encoded structural elements involved in pseudohyphal growth (Fig. 6a). The expression of transcripts related to ribonucleoprotein complex-localization, cytoplasm-localization, and membrane-localization were dramatically altered. Of 39 altered transcripts related to ribonucleoprotein complex-localization, 36 were downregulated, accounting for 92% of the total. In addition, over 40% of membrane-localization transcripts that exhibited altered expression encoded transporters were responsible for transporting sugars, choline and H^+. In addition to nuclear, cytosol, and mitochondrion-localized transcripts, all transcripts involved in cytoskeleton-localization were indeed upregulated during pseudohyphal growth (Fig. 6a). These upregulated transcripts included those that encode MOB1/2, G2 mitotic-specific cyclin B, myosin, and kinesin. The upregulated GG4282|c32_g1_i1 and GG4282|c36_g1_i1 transcripts that encode MOB1/2

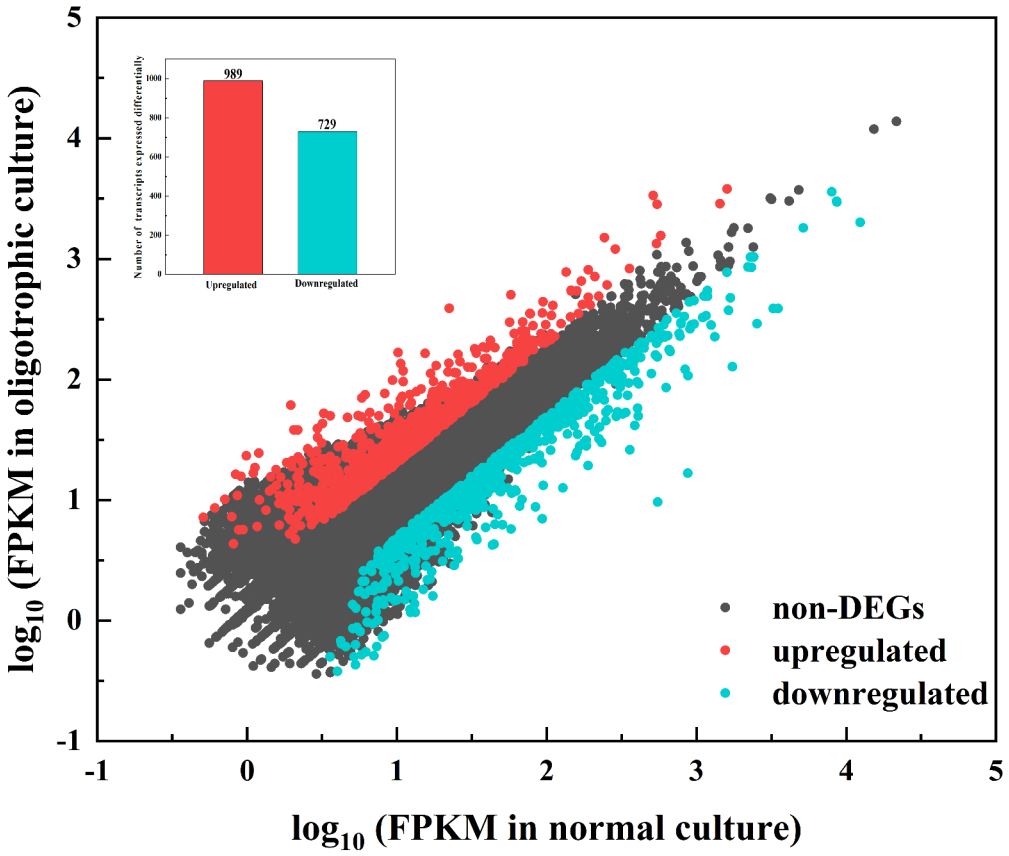

Fig. 5 The expressional comparison of transcripts in *U. muehlenbergii* between normal cultivation and oligotrophic cultivation. Each point represents a transcript. The x- and y-axis are the $\log_{10}$ of the normalized expression level (FPKM) of transcripts *in U. muehlenbergii* at normal and oligotrophic cultivation. The transcripts with significant change at the absolute value of $\log_2$ (FPKM ratio in two cultivation) ≥ 1 and FDR ≤ 0.05 were shown in red and green points. Red points were upregulated and green points were downregulated transcripts. Black points indicate non-differentially expressed genes (non-DEG). The inserted figure showed the number of upregulated and downregulated transcripts

simultaneously belonged to the GO-septin cytoskeleton organization category. Myosin and kinesin encoded by GG5341|c5_g1_i1, GG3061|c5_g1_i1, and GG9552|c84_g1_i1 interact together to produce chitin synthase that is responsible for cell wall synthesis during hyphal elongation (Schuster et al. 2012).

Within the GO-molecule function category (Fig. 6b), transcriptomic changes of enzymes involved in oligotrophic stress were particularly assessed. In addition to the catalytic activity category, the three most prominent categories exhibiting transcriptional changes for specific enzymes were those with hydrolase, transferase, and oxidoreductase activities (Fig. 6b). Some downregulated transcripts within these categories were associated with hydrolyzing glucan, which is an important fungal cell wall component. For example, downregulated transcripts within the hydrolase category, including GG3772|c0_gl_i1, GG3772|c2_gl_i1, GG7279|c121_gl_i1, and GG3862|c3_gl_i1, encoded glucanases that are cell wall degrading enzymes that hydrolyze cell wall glucan. Downregulated transcripts within the oxidoreductase category like GG7971|c0_gl_i1 encoded glycoside hydrolases that hydrolyze broad polysaccharide or glycan substrates.

Environmental stress from oligotrophic cultivation can induce oxidative stress in living cells that accompany the generation of reactive oxygen species (ROS). Thus, transcripts encoding oxidoreductases that exhibited altered expression were particularly evaluated (Fig. 6b). Among these, transcripts encoding oxidases, dioxygenases, and cloroperoxidases were upregulated, while transcripts encoding

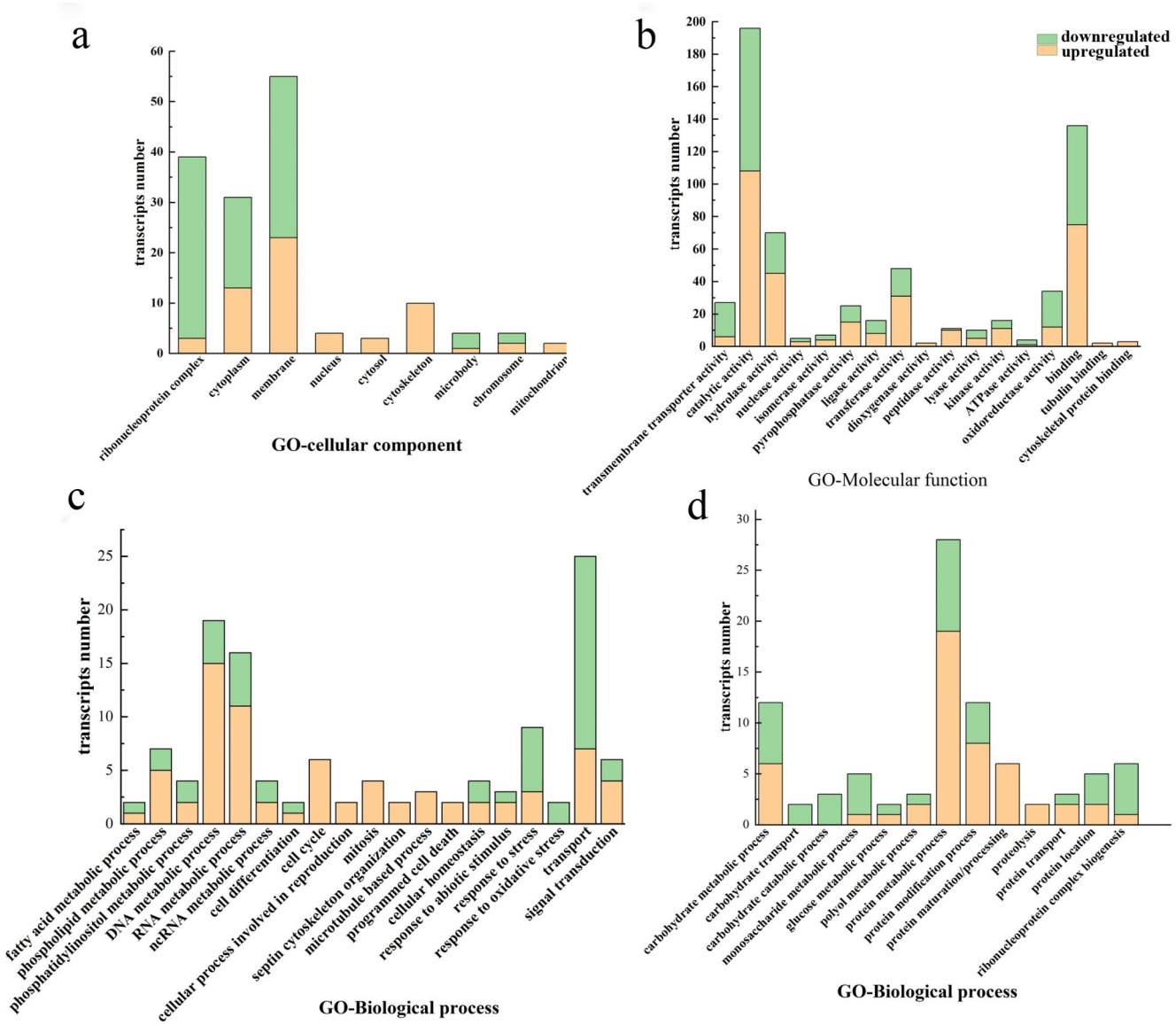

Fig. 6 Gene ontology classifications of upregulated and downregulated transcripts in *U. muehlenbergii* under oligotrophic stress. GO categories assigned to the *U. muehlenbergii* transcriptome was classified into three categories: cellular components, molecular functions, and biological processes

catalases, dehydrogenases, uricases, FAN/FMN binding proteins, and thioredoxins were downregulated. In addition, transcripts encoding diverse reductases exhibited upregulation or downregulation. Notably, three transcripts encoding important mediators of oxidative stress were downregulated including GG6871|c2_g1_i1 (lyase: glutathione-dependent formaldehyde-activating enzyme), GG8258|c2_g1_i1 (hydrolase: hydroxyacylglutathione hydrolase), and GG7102|c62_g1_i1 (transferase: glutathione S-transferase). The enzymes encoded by these downregulated transcripts play important roles in detoxication and can eliminate by-products from oxidative stress. In addition, the transcripts GG9086|c0_g1_i1 and GG9086|c2_g1_i1 which encode thioredoxin and play cytoprotective roles against various oxidative stresses were downregulated. Further, GG1583|c6_g1_i1 encodes catalase, an important antioxidant enzyme involved in ROS processing that prevents cellular oxidant damage, and was also downregulated. Lastly, GG8944|c3_g1_i1 encodes peroxidase, an oxidase that catalyzes the oxidation of organic compounds and was upregulated.

In addition to the transcripts described above, numerous transcripts that encode enzymes like kinases, pyrophosphatases, ligases, and peptidases exhibited altered expression when *U. muehlenbergii* was grown under oligotrophic conditions (Fig. 6b). Further, the most abundant category,

the catalytic activity group, also contained transcripts with unclassified enzymes involved in oligotrophic stress, including the downregulated gene GG7964|c183_g1_i1 (polyketide synthase) that is responsible for producing secondary metabolite polyketides in fungi.

Fungal pseudohyphal growth is inevitably accompanied by supplementation and delivery of membrane and cytoskeleton components. Unsurprisingly, some transcripts involved in cytoskeletal protein binding and transmembrane transporter activity exhibited altered patterns in the pseudohyphal state of *U. muehlenbergii* (Fig. 6b). Furthermore, GO-biological process analysis also revealed the presence of some transcripts with an altered expression, which were associated with compound transport (Fig. 6c). Moreover, transcripts associated with carbohydrate transport were downregulated (Fig. 6d).

Under oligotrophic conditions, transcripts associated with DNA/RNA metabolism also exhibited considerably altered transcriptional expression (Fig. 6c). Specifically, transcripts associated with DNA replication were all upregulated. In addition, transcripts involved in the cell cycle, cellular processes involved in reproduction, mitosis, septin cytoskeleton organization, microtubule-based processes, and programmed cell death were all upregulated (Fig. 6c). Among GO-cellular processes involved in reproduction categories, some transcripts were associated with fungal hyphal growth, like the *MAT 1-1-1* and cell division control protein (CDC) genes (Bohm et al. 2013; Yong et al. 2020). Specifically, GG8782|c2_g1_i1 (mating-type protein MAT1-1-1) and GG9760|c1_g1_i1 (cell division control protein) were upregulated.

GO-biological process analysis also revealed the presence of some transcripts with altered expression that were involved in carbohydrate and protein metabolic processes (Fig. 6d). These included transcripts annotated to be involved in protein modification, maturation/processing, proteolysis, transport, and location. Most of the transcripts involved in ribonucleoprotein complex biogenesis exhibited downregulated expression. Further, a considerable number of transcripts involved in carbohydrate transport and catabolic processes, monosaccharide catabolism were downregulated.

KEGG analysis of transcripts with altered expression

To complement the GO analysis and obtain more information regarding the metabolic pathways of *U. muehlenbergii* affected by oligotrophic conditions, KEGG functional enrichment analysis was conducted (Fig. 7). After excluding some redundant pathways, a total of 42 KEGG pathways within six categories were represented by transcripts with significantly altered expression levels (Fig. 7). Overall, 18 KEGG pathways were enriched among upregulated transcripts during oligotrophic conditions, including those involved in the cell cycle (yeast) and meiosis (yeast), various N-glycan biosynthesis processes, and glycosaminoglycan degradation pathways associated with glycan, SNARE interactions within the vesicular transport pathway associated with membrane fusion, the TCA cycle, and common metabolic pathways for the complete oxidation of carbohydrates, proteins, and fats. Only eight enriched KEGG pathways were associated with downregulated transcripts,

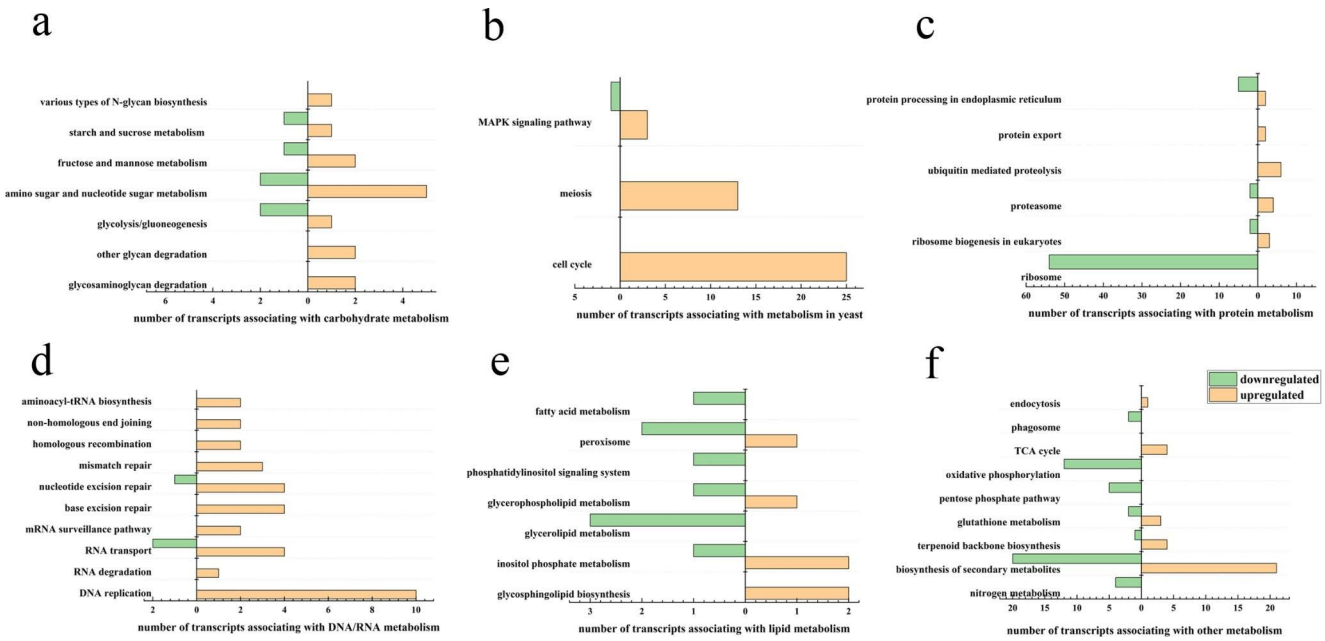

Fig. 7 KEGG classifications of upregulated and downregulated transcripts in *U. muehlenbergii* under oligotrophic stress

including those involved in ribosome functioning, oxidative phosphorylation, and the pentose phosphate pathway. In addition, 16 KEGG pathways that were enriched contained both upregulated and downregulated transcripts. The enriched pathway with the most striking upregulated transcripts was the cell cycle (yeast), while the pathway with the most striking downregulated transcripts was ribosome functioning (Fig. 7b and c).

The cell-cycle (yeast) pathway (Fig. 7b**)** encompassed several upregulated transcripts associated with maintenance and segregation of chromosomes, DNA biosynthesis and repair, release from the nucleolus, and cell cycle arrest. For instance, the upregulated gene GG3173|C3_g1_i1 encoded the mini-chromosome maintenance DNA-dependent ATPase, while the upregulated gene GG4198|C1_g1_i1 encoded the chromosome segregation protein. In addition, several upregulated transcripts encoded cell division control proteins (CDC) and cyclin-dependent protein kinases (CDK) including GG9760|c2_g1_i1, GG9760|c1_g1_i1, and GG7546|c3_g1_i1. These proteins are involved in controlling fungal cell division and modulating their transcription. Within the cell-cycle pathway, some upregulated transcripts (e.g., Dbf4: GG9511| c0_g1_i1, GG9511| c3_g1_i, and GG9511| c6_g1_i1) encoded protein kinases containing conserved class I zinc finger domains (C_2H_2). A previous study observed that the transcription factor (Mig1) with the C_2H_2 domain favored filamentous growth of *S. cerevisiae* when searching for alternative carbon sources (Karunanithi and Cullen 2012). Some upregulated transcripts of *U. muehlenbergii* under the oligotrophic conditions of this study also harbored C_2H_2 domains. Nevertheless, it is unclear whether these upregulated transcripts with C_2H_2 domains are related to pseudohyphal growth of *U. muehlenbergii*.

The upregulated transcripts, GG9760|c2_g1_i1 (cyclin), GG4282|c32_g1_i1, and GG4282|c36_g1_i1 (MOB1/2) were associated with the cell-cycle (yeast) pathway, but also GO-cytoskeleton localization. Further, the number of upregulated transcripts within the G2 and M phases was clearly larger than those for the G1 and S phases (Supplemental Fig. 2). Transcripts encoding CIb1/2 and CDC28 were simultaneously upregulated and are involved in the critical site for mediating cell cycle arrest and entering a mitotic exit. The G2 phase is elongated and the G1 phase is diminished in yeast pseudohyphae cells (Kron et al. 1994). Thus, the results of this study provide insights into the unique transcriptional expression involved in the checkpoint of the *U. muehlenbergii* pseudohypal cell cycle. Greater numbers of upregulated transcripts in the G2 and M phase, in addition to the presence of upregulated transcripts in the critical site of the cell cycle are probably associated with elongated G2 phases.

The MAPK pathway commonly controls filamentous growth in yeast. Four MAPK transcripts exhibited altered expression during psedudohyphal of *U. muehlenbergii* (Fig. 7b) including upregulated GG4810|c1_g1_i1 (mitogen-activated protein kinase), GG8881|c5_g1_i1 (Ras-GTPase), and GG1089|c2_g1_i1 (Bem1 protein kinase activator), in addition to downregulated GG1583|c6_g1_i1 (catalase). Further, transcripts involved in the biosynthesis of secondary metabolites exhibited altered expression under oligotrophic growth (Fig. 7f). Further, several transcripts involved in carbohydrate metabolism pathways were upregulated, including those involved in amino sugar and nucleotide sugar metabolism, N-glycan biosynthesis, general glycan degradation, and glycosaminoglycan degradation (Fig. 7a). Transcripts involved in DNA replication also exhibited upregulated expression levels. Several transcripts associated with RNA transport and aminoacyl-tRNA biosynthesis were induced by oligotrophic cultivation (Fig. 7d). Most of these upregulated transcripts encoded types of DNA polymerases, RNA polymerases, tRNA synthases, and translation initiation factors. Moreover, diverse transcripts associated with repair mechanisms were unsurprisingly upregulated due to oligotrophic cultivation.

Within the most strikingly downregulated KEGG ribosome pathway, all transcripts encoding the ribonucleoprotein complex were dramatically downregulated during oligotrophic growth (Fig. 7c). Stressful conditions, and especially nutritional starvation, can lead to obvious decreases in the expression of transcripts encoding ribosomal proteins in bacteria and other fungi (Jona et al. 2000; Cantwell et al. 1992; Ghulam et al. 2020). Thus, downregulation of ribonucleoproteins due to stress may be a universal phenomenon. Indeed, the downregulation of ribonucleoprotein transcripts may be a sensitive indicator for general stress conditions. In addition to downregulated ribonucleoprotein transcripts, transcripts involved in oxidative phosphorylation and the pentose phosphate pathway were also downregulated, suggesting the presence of metabolic adjustments during pseudohyphal growth of *U. muehlenbergii*, including variation in ATP and NADPH synthesis. In addition, the reduced strength of the PDA medium used in this study also likely limited nitrogen source availability. Accordingly, four transcripts associated with nitrogen metabolism were also downregulated under oligotrophic conditions (Fig. 7f). Some transcripts involved in glycerolipid metabolism were also downregulated (Fig. 7e), while several transcripts involved in glycolysis, in addition to amino sugar and nucleotide sugar metabolism were downregulated (Fig. 7a).

Discussion

Under available partially complete genomic information of *Umbilicria muehlenbergii* published in GenBank, our RNA-seq research provided about 22 million transcriptional reads and assembled the transcriptome of *U. muehlenbergii*. Thus, the study represents the most comprehensive transcriptomic data yet available for *U. muehlenbergii* and supplements the available accurate genome information, while serving as a foundation for further functional genomics research of *U. muehlenbergii*. Specifically, the RNA-seq data described here may provide a foundation for analyzing non-coding RNAs, the identification of new genes, and future assembly and annotation of *U. muehlenbergii* genomes. Further, transcripts of *U. muehlenbergii* exhibiting altered expression under oligotrophic conditions were identified here, while biological pathways affected by these conditions were also evaluated. These results are thus beneficial for understanding molecular mechanisms underlying the yeast and pseudohyphal transitions of *U. muehlenbergii*. In addition, we evaluated the distribution of SSRs from *U. muehlenbergii* and reported GO classification of unigene-derived SSRs under oligotrophic stress. The results are valuable for choice of genetic marker and understanding adaptive traits of *U. muehlenbergii*.

The morphological study confirmed that oligotrophic stress and polyols addition induced pseudohyphal growth of *U. muehlenbergii*. In lichens, various polyols producing from symbiotic algae are transferred to mycobionts fungi, thereby supporting their growth and reproduction (Wang et al. 2014; Meena et al. 2015). For example, the lichen-forming fungi *Endocarpon pusillum* preferentially absorbs sorbitol and mannitol (Wang et al. 2014). The photobionts of *U. muehlenbergii* and *Endocarpon pusillum* are belonging to the green algal genera *Trebouxia* and *Diplosphaera*, respectively, and therefore, it remains unclear whether *U. muehlenbergii* photobionts could directly produce polyols as *Endocarpon pusillum*. The morphological study showed that there was the most obvious pseudohyphal growth of *U. muehlenbergii* in oligotrophic medium supplemented with mannitol and sorbitol (Fig. 1), and the transcriptomic data showed that transcripts encoding sorbitol dehydrogenase and sorbitol transporter were upregulation, both of which suggesting that *U. muehlenbergii* could assimilate and metabolize sorbitol as the alternative carbon source to support their pseudohyphal elongation. In natural systems, mannitol and sorbitol may be the primary photosynthetic products transferred from lichen photobionts to lichen-forming fungi. Herein, we propose that pseudohyphal formation in *U. muehlenbergii* may be an adaptive mechanism by which *U. muehlenbergii* survives in oligotrophic environments, because lichen-forming fungi *U. muehlenbergii* with elongated pseudohypha could have greater opportunities to capture their photobiont partners and survive in stress environment. In one word, the pseudohyphal form of lichen-forming fungi is more favorable for identifying algal partners, interacting with the photosynthetic organism and increasing the efficiency of carbohydrate uptake from the photobiont.

Overall, several general conclusions and speculations can be drawn from the present transcriptomic study. First, GO and KEGG pathway analysis revealed that ribonucleoproteins were severely downregulated in oligotrophic stress. Previous phosphoproteomic studies have shown that phosphorylation of ribonucleoproteins plays important roles in yeast pseudohyphal growth (Shively et al. 2015). Our results further indicate that downregulation of ribonucleoproteins also is stress indicator for fungus pseudohyphal state at transcriptomic level.

Second, pseudohyphal growth of *U. muehlenbergii* were accompanied with abundant metabolic changes in oligotrophic stress. Both KEGG and GO analysis had shown that pathways associating with carbohydrate, protein, DNA/RNA and lipid metabolism were enriched remarkably, and that the corresponding transporters carrying on biomacromolecules were enriched. The results suggested that DNA replication, RNA transcription, protein, carbohydrate and lipid synthesis and degradation were highly required and active in pseudohyphal growth of *U. muehlenbergii*, although the oligotrophic medium just supply scarce nutrients. Pseudohyphal growth was a developmental process of live cells, in which diverse metabolic enzymes were required for balancing the relationship between growth and proliferation. As observed from GO-cellular component, the diverse metabolic enzymes were enriched in the corresponding enzymatic category, such as hydrolases, transferases, oxidoreductases, and other enzymes. In addition, KEGG analysis showed that biosynthesis of secondary metabolites pathway was enriched, suggesting that there were probably unusual metabolic products involving in stress-tolerance during pseudohyphal growth of *U. muehlenbergii*.

Third, the pseudohyphal growth of *U. muehlenbergii* requires continuous support from cytoskeletal and membrane structure. GO-cellular component clearly showed that membrane- and cytoskeleton-localization, septin cytoskeleton organization, microtubule-based processes were significantly enriched. In addition, KEGG analysis showed the most enriched cell cycles pathway, which closely controlled cell adhesion and cell cytoskeleton, indicating that cytoskeleton components are active at the transcriptional level during pseudohyphal growth of *U. muehlenbergii*. The pseudohyphal growth in fungi also requires recycling and transporting membrane lipid and protein, which were delivered by motors along the cytoskeleton to the pseudohyphal

apex. By KEGG and GO analysis, the pathways related with the process mentioned above were indeed apparently enriched, such as "SNARE interactions within the vesicular transport" pathway, protein and glycerolipid metabolism.

Finally, synergistic cooperation from multiple biological pathways helps *U. muehlenbergii* to survive under oligotrophic stress. Oligotrophic stress signal activates MAPK pathway, and then, the latter triggers cell cycle and meiosis pathway, transcriptomic changes of which were indeed detected. KEGG analysis showed apparently enriched TCA cycle, pentose phosphate pathway and oxidative phosphorylation pathways, suggesting that metabolic reconstruction occurred in *U. muehlenbergii* under oligotrophic stress with high concentration of sorbitol. The transcriptomic change of these pathways was more favorable for survival of *U. muehlenbergii* by adjusting energy metabolism when sorbitol was alternative carbon sources. The response to stress and response to oxidative stress in GO and mismatch repair pathway in KEGG were apparently enriched, which contained plenty of transcripts encoding oxidoreductase, catalases, thioredoxins and glutaredoxin, which were well-known antioxidant enzymes. Under oligotrophic stress, the activation of the pathways involved in producing protectants could protect *U. muehlenbergii* from oxidative stress deriving from high concentration of sorbitol.

However, a total of 811 transcripts with altered expression remained uncharacterized in our analyses, accounting for 47.2% (811/1718) of the total transcripts with altered expression, likely due to minimal knowledge of lichen-forming fungal genomes. The lack of characterization for these transcripts still limited understanding of the molecular mechanism underlying pseudohyphal growth. Thus, additional refined annotation of the *U. muehlenbergii* genome is needed in the future. Nevertheless, this study revealed that nutrient status plays a key role in dimorphic transition in *U. muehlenbergii*, which is yeast-like morphologies under rich nutrient conditions and pseudohyphal morphologies under nutrient stress. In addition, since the transcriptional responses of living cells to stimuli are transient, the transcriptional responses of *U. muehlenbergii* at different developmental stages should be explored in the future.

Supplementary Information The online version contains supplementary material available at https://doi.org/10.1007/s11274-023-03618-z.

Acknowledgements We are indebted to Miss Hui Li for help in taking pictures of mycelial morphology. This work was supported by the National Natural Science Foundation of China (grant number 41906201).

Author Contributions Dongjie Fan, Chuanpeng Liu and Qiming Zhou contributed to the study conception and design. Material preparation, data collection and analysis were performed by Dongjie Fan, Lushan Liu and Rui Liao. The biological resource was provided by Shunan Cao. The first draft of the manuscript was written by Dongjie Fan. Qiming Zhou and Chuanpeng Liu commented on and revised previous versions of the manuscript. All authors read and approved the final manuscript.

Declarations

Competing interests The authors have no relevant financial or non-financial interests to disclose.

References

Aubert S, Juge C, Boisson AM, Gout E, Bligny R (2007) Metabolic processes sustaining the reviviscence of lichen Xanthoria elegans (Link) in high mountain environments. Planta 226:1287–1297

Bohm J, Hoff B, O'Gorman CM, Wolfers S, Klix V, Binger D, Zadra I, Kurnsteiner H, Poggeler S, Dyer PS, Kuck U (2013) Sexual reproduction and mating-type-mediated strain development in the penicillin-producing fungus Penicillium chrysogenum. Proc Natl Acad Sci U S A 110:1476–1481

Bolger AM, Lohse M, Usadel B (2014) Trimmomatic: a flexible trimmer for Illumina sequence data. Bioinformatics 30:2114–2120

Brunauer G, Hager A, Krautgartner WD, Turk R, Worgotter ES (2006) Experimental studies on Lecanora rupicola (L.) Zahlbr.: chemical and microscopical investigations of the mycobiont and re-synthesis stages. Lichenologist 38:577–585

Brunauer G, Hager A, Grube M, Turk R, Stocker-Worgotter E (2007) Alterations in secondary metabolism of aposymbiotically grown mycobionts of Xanthoria elegans and cultured resynthesis stages. Plant Physiol Biochem 45:146–151

Cantwell R, McEntee CM, Hudson AP (1992) Regulation of mitochondrial transcription during the stringent response in yeast. Curr Genet 21:241–247

Cullen PJ, Sabbagh W, Graham E, Irick MM, van Olden EK, Neal C, Delrow J, Bardwell L, Sprague GF (2004) A signaling mucin at the head of the Cdc42- and MAPK-dependent filamentous growth pathway in yeast. Genes Dev 18:1695–1708

Elshobary ME, Osman ME, Abo-Shady AM, Komatsu E, Perreault H, Sorensen J, Piercey-Normore MD (2016) Algal carbohydrates affect polyketide synthesis of the lichen-forming fungus Cladonia rangiferina. Mycologia 108:646–656

Ghulam MM, Catala M, Abou Elela S (2020) Differential expression of duplicated ribosomal protein genes modifies ribosome composition in response to stress. Nucleic Acids Res 48:1954–1968

Hirabayashi K, Iwata S, Ito M, Shigeta S, Narui T, Mori T, Shibata S (1989) Inhibitory effect of a lichen polysaccharide sulfate, GE-3-S, on the replication of human immunodeficiency virus (HIV) in vitro. Chem Pharm Bull (Tokyo) 37:2410–2412

Jin R, Dobry CJ, McCown PJ, Kumar A (2008) Large-scale analysis of yeast filamentous growth by systematic gene disruption and overexpression. Mol Biol Cell 19:284–296

Jona G, Choder M, Gileadi O (2000) Glucose starvation induces a drastic reduction in the rates of both transcription and degradation of mRNA in yeast. Biochim Biophys Acta 1491:37–48

Karunanithi S, Cullen PJ (2012) The filamentous growth MAPK pathway responds to glucose starvation through the Mig1/2 transcriptional repressors in Saccharomyces cerevisiae. Genetics 192:869–887

Karunanithi S, Vadaie N, Chavel CA, Birkaya B, Joshi J, Grell L, Cullen PJ (2010) Shedding of the mucin-like flocculin Flo11p reveals a new aspect of fungal adhesion regulation. Curr Biol 20:1389–1395

Kron SJ, Styles CA, Fink GR (1994) Symmetric cell division in pseudohyphae of the yeast Saccharomyces cerevisiae. Mol Biol Cell 5:1003–1022

Kuchin S, Vyas VK, Carlson M (2002) Snf1 protein kinase and the repressors Nrg1 and Nrg2 regulate FLO11, haploid invasive growth, and diploid pseudohyphal differentiation. Mol Cell Biol 22:3994–4000

Liu Y, Xie L, Gong G, Zhang W, Zhu B, Hu Y (2014) De novo comparative transcriptome analysis of Acremonium chrysogenum: high-yield and wild-type strains of cephalosporin C producer. PLoS ONE 9:e104542

Lorenz MC, Cutler NS, Heitman J (2000) Characterization of alcohol-induced filamentous growth in Saccharomyces cerevisiae. Mol Biol Cell 11:183–199

Madhani HD (2000) Interplay of intrinsic and extrinsic signals in yeast differentiation. Proc Natl Acad Sci U S A 97:13461–13463

Mao X, Cai T, Olyarchuk JG, Wei L (2005) Automated genome annotation and pathway identification using the KEGG Orthology (KO) as a controlled vocabulary. Bioinformatics 21:3787–3793

Marcel M (2011) Cutadapt removes adapter sequences from high-throughput sequencing reads. EMBnet J 17:10–12

Meena M, Prasad V, Zehra A, Gupta VK, Upadhyay RS (2015) Mannitol metabolism during pathogenic fungal-host interactions under stressed conditions. Front Microbiol 6:1019

Molnar K, Farkas E (2010) Current results on biological activities of lichen secondary metabolites: a review. Z Naturforsch C J Biosci 65:157–173

Palmqvist K (2000) Tansley Review No. 117: Carbon economy in lichens. New Phytol 148:11–36

Pan X, Heitman J (1999) Cyclic AMP-dependent protein kinase regulates pseudohyphal differentiation in Saccharomyces cerevisiae. Mol Cell Biol 19:4874–4887

Park SY, Jeong MH, Wang HY, Kim JA, Yu NH, Kim S, Cheong YH, Kang S, Lee YH, Hur JS (2013) Agrobacterium tumefaciens-mediated transformation of the lichen fungus, Umbilicaria muehlenbergii. PLoS ONE 8:e83896

Park SY, Choi J, Lee GW, Jeong MH, Kim JA, Oh SO, Lee YH, Hur JS (2014) Draft genome sequence of Umbilicaria muehlenbergii KoLRILF000956, a Lichen-Forming Fungus Amenable to genetic manipulation. Genome Announc 2.

Richardson DH, Smith DC, Lewis DH (1967) Carbohydrate movement between the symbionts of lichens. Nature 214:879–882

Robinson MD, McCarthy DJ, Smyth GK (2010) edgeR: a Bioconductor package for differential expression analysis of digital gene expression data. Bioinformatics 26:139–140

Ryan O, Shapiro RS, Kurat CF, Mayhew D, Baryshnikova A, Chin B, Lin ZY, Cox MJ, Vizeacoumar F, Cheung D, Bahr S, Tsui K, Tebbji F, Sellam A, Istel F, Schwarzmuller T, Reynolds TB, Kuchler K, Gifford DK, Whiteway M, Giaever G, Nislow C, Costanzo M, Gingras AC, Mitra RD, Andrews B, Fink GR, Cowen LE, Boone C (2012) Global gene deletion analysis exploring yeast filamentous growth. Science 337:1353–1356

Schuster M, Treitschke S, Kilaru S, Molloy J, Harmer NJ, Steinberg G (2012) Myosin-5, kinesin-1 and myosin-17 cooperate in secretion of fungal chitin synthase. EMBO J 31:214–227

Shively CA, Kweon HK, Norman KL, Mellacheruvu D, Xu T, Sheidy DT, Dobry CJ, Sabath I, Cosky EE, Tran EJ, Nesvizhskii A, Andrews PC, Kumar A (2015) Large-scale analysis of kinase signaling in yeast Pseudohyphal Development identifies regulation of Ribonucleoprotein Granules. PLoS Genet 11:e1005564

Spribille T, Resl P, Stanton DE, Tagirdzhanova G (2022) Evolutionary biology of lichen symbioses. New Phytol 234:1566–1582

Stepanenko SL, Maksimov O, Fedoreev SA, Miller G (1998) Polysaccharides of lichens and their sulfated derivatives: antiviral activity. Chem Nat Compd 34:337–338

Wang YY, Liu B, Zhang XY, Zhou QM, Zhang T, Li H, Yu YF, Zhang XL, Hao XY, Wang M, Wang L, Wei JC (2014) Genome characteristics reveal the impact of lichenization on lichen-forming fungus endocarpon pusillum Hedwig (Verrucariales, Ascomycota). BMC Genomics 15:34

Wang Y, Wei X, Bian Z, Wei J, Xu JR (2020) Coregulation of dimorphism and symbiosis by cyclic AMP signaling in the lichenized fungus Umbilicaria muhlenbergii. Proc Natl Acad Sci U S A 117:23847–23858

Yong M, Yu J, Pan X, Yu M, Cao H, Song T, Qi Z, Du Y, Zhang R, Yin X, Liu W, Liu Y (2020) Two mating-type genes MAT1-1-1 and MAT1-1-2 with significant functions in conidiation, stress response, sexual development, and pathogenicity of rice false smut fungus Villosiclava virens. Curr Genet 66:989–1002

Zakeri Z, Junne S, Jager F, Dostert M, Otte V, Neubauer P (2022) Lichen cell factories: methods for the isolation of photobiont and mycobiont partners for defined pure and co-cultivation. Microb Cell Fact 21:80

Zhang HK, Lu H, Wang J, Liu GF, Zhou JT, Xu MY (2013) Global transcriptome analysis of Escherichia coli exposed to immobilized anthraquinone-2-sulfonate and azo dye under anaerobic conditions. Appl Microbiol Biotechnol 97:6895–6905

Zhu S, Cao YZ, Jiang C, Tan BY, Wang Z, Feng S, Zhang L, Su XH, Brejova B, Vinar T, Xu M, Wang MX, Zhang SG, Huang MR, Wu R, Zhou Y (2012) Sequencing the genome of Marssonina brunnea reveals fungus-poplar co-evolution. BMC Genomics 13:382